Quantitative biochemical rationale for differences in transmissibility of 1918 pandemic influenza A viruses

Aravind Srinivasan[†], Karthik Viswanathan[†], Rahul Raman[†], Aarthi Chandrasekaran[†], S. Raguram[†], Terrence M. Tumpey[‡], V. Sasisekharan[§], and Ram Sasisekharan[‡§¶‖]

[†]Department of Biological Engineering, [§]Harvard-Massachusetts Institute of Technology Division of Health Sciences and Technology, and [¶]Center for Cancer Research, Massachusetts Institute of Technology, Cambridge, MA 02139; and [‡]Influenza Division, National Center for Immunization and Respiratory Diseases, Coordinating Center for Infectious Diseases, Centers for Disease Control and Prevention, Mailstop G-16, 1600 Clifton Road NE, Atlanta, GA 30333

Communicated by Robert Langer, Massachusetts Institute of Technology, Cambridge, MA, December 19, 2007 (received for review December 2, 2007)

The human adaptation of influenza A viruses is critically governed by the binding specificity of the viral surface hemagglutinin (HA) to long (chain length) α2-6 sialylated glycan (α2-6) receptors on the human upper respiratory tissues. A recent study demonstrated that whereas the 1918 H1N1 pandemic virus, A/South Carolina/1/1918 (SC18), with α2-6 binding preference transmitted efficiently, a single amino acid mutation on HA resulted in a mixed α2-3 sialylated glycan (α2-3)/α2-6 binding virus (NY18) that transmitted inefficiently. To define the biochemical basis for the observed differences in virus transmission, in this study, we have developed an approach to quantify the multivalent HA–glycan interactions. Analysis of the molecular HA–glycan contacts showed subtle changes resulting from the single amino acid variations between SC18 and NY18. The effect of these changes on glycan binding is amplified by multivalency, resulting in quantitative differences in their long α2-6 glycan binding affinities. Furthermore, these differences are also reflected in the markedly distinct binding pattern of SC18 and NY18 HA to the physiological glycans present in human upper respiratory tissues. Thus, the dramatic lower binding affinity of NY18 to long α2-6 glycans, as against a mixed α2-3/6 binding, correlates with its inefficient transmission. In summary, this study establishes a quantitative biochemical correlate for influenza A virus transmission.

hemagglutinin | multivalency | sialylated glycans

The Spanish influenza pandemic of 1918 caused by the H1N1 subtype virus resulted in ≈20 million to 50 million deaths worldwide (1). The emergence of avian influenza H5N1 viruses that are able to infect humans (>300 known cases) and produce a high mortality rate (≈200 deaths) has raised serious global health concerns. Significantly, adaptation of these viruses for efficient human–human transmission could result in a new influenza pandemic, a public health disaster of tragic proportions.

The critical step in the host infection of influenza viruses is the binding of their viral surface hemagglutinin (HA) to sialylated glycan receptors on the epithelial cell surface of the host organism (2–6). The evolution of pandemic viruses involves crossing-over of avian influenza viruses (natural host) to humans and adaptation to the human host for subsequent infection and human–human transmission (2, 7). This cross-over is believed to involve mutations in HA that switch its glycan receptor preference from α2-3 sialylated (α2-3) to α2-6 sialylated (α2-6) glycans found in abundance in human upper respiratory epithelia (3–5, 8). The human upper respiratory tract α2-6 receptor adaptation of HA is a critical step in permitting the viruses to infect and efficiently replicate in these tissues, leading to rapid human–human transmission (8). Several studies have been performed to elucidate the distribution of glycans in human upper respiratory tissues (4, 8–10). We recently demonstrated that human upper airways express a diversity of α2-6 structures with a predominant expression of long oligosaccharides (11). More importantly, we observed that both α2-3 and short α2-6 glycan structures adopt a distinct, narrow cone-like topology, whereas long α2-6 glycans adopt a flexible umbrella-like topology. Human-adapted H1 and H3 HA demonstrated high-affinity binding specificity to long α2-6 glycans that are expressed in the human upper respiratory epithelium. The classification of HA glycan specificity in terms of the glycan topology instead of the linkage has permitted us to distinguish the observed α2-3 and α2-6 binding of avian HAs from that of the α2-6 binding of human-adapted HA. Based on these observations, we postulated that HA specificity to α2-6 glycan receptors with distinct topology is the critical determinant for efficient human adaptation of HA (11).

The relationship between HA mutations, which lead to a change in glycan receptor preference and transmissibility of the prototypic 1918 H1N1 pandemic virus [A/South Carolina/1/1918 (SC18)] has been investigated by using the ferret model (12). Recently, Tumpey *et al.* (12) demonstrated that the SC18 with α2-6 binding preference transmitted efficiently but a single amino acid HA mutation (SC18 + one mutation) resulted instead in a mixed α2-3/α2-6 binding virus (NY18) that transmitted inefficiently. Furthermore, a second HA mutation (NY18 + one mutation) resulted in an α2-3 binding virus (AV18) that did not transmit. This model system is ideally suited to study transmissibility purely based on HA mutations, as all other genes are identical in the different viruses. These remarkable differences in virus transmission as the result of a single amino acid mutation on HA, in turn, raise important questions about HA-glycan specificity in the context of glycan topology not only for human adaptation but also for efficient transmission.

In this study, we have developed a quantitative framework to investigate HA–glycan specificity to explain the observed differences in the transmissibility of the 1918 pandemic influenza A viruses. The differences in the molecular HA–glycan contacts caused by the single amino acid variations were investigated by using H1 HA–glycan cocrystal structures (13). The effects of these subtle differences on the multivalent HA–glycan interactions were captured by using a quantitative glycan-binding assay to establish the relative glycan binding affinities of the HAs. The physiological relevance of the differences in the HA–glycan binding affinities was investigated by using HA binding to human upper respiratory tissues. Taken together, this approach establishes a quantitative biochemical correlation between influenza virus HA–glycan binding and virus transmission.

Author contributions: A.S., K.V., R.R., and A.C. contributed equally to this work; V.S., R.R., and R.S. designed research; A.S., K.V., R.R., A.C., and S.R. performed research; A.S., A.C., and T.M.T. contributed new reagents/analytic tools; A.S., K.V., R.R., A.C., S.R., T.M.T., and R.S. analyzed data; and R.R., V.S., and R.S. wrote the paper.

The authors declare no conflict of interest.

Freely available online through the PNAS open access option.

‖To whom correspondence should be addressed. E-mail: rams@mit.edu.

This article contains supporting information online at www.pnas.org/cgi/content/full/0711963105/DC1.

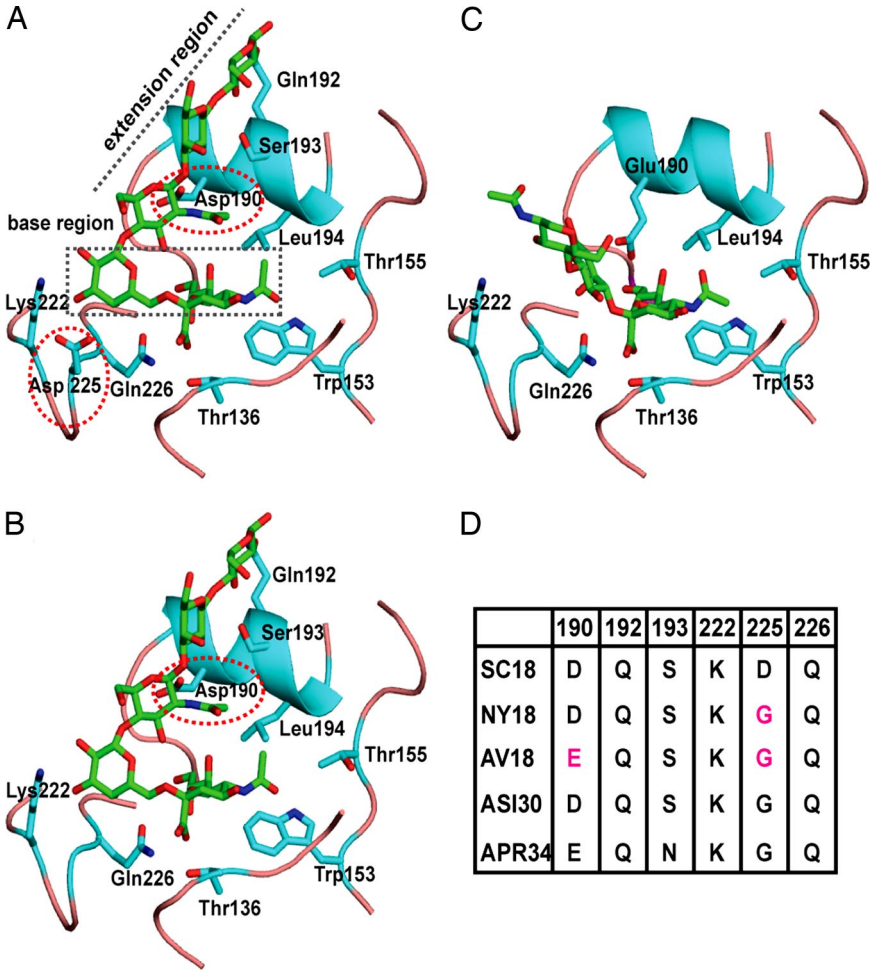

D

	190	192	193	222	225	226
SC18	D	Q	S	K	D	Q
NY18	D	Q	S	K	G	Q
AV18	E	Q	S	K	G	Q
ASI30	D	Q	S	K	G	Q
APR34	E	Q	N	K	G	Q

Fig. 1. Molecular interactions of SC18, NY18, and AV18 HAs with α2-3 and α2-6. The glycan binding site on HA is shown with the critical amino acids including the highly conserved Neu5Ac anchors (Thr-136, Trp-153, Thr-155, and Leu-194). Tyr-95 and His-183 are not shown for clarity. The amino acid positions are numbered based on H1N1 HA. (*A*) Shown is the interaction of the SC18 HA with long α2-6 in the umbrella-like topology. Lys-222, Asp-225, and Gln-226 provide critical contacts with the base region, and Asp-190, Gln-192, and Ser-193 provide optimal contacts with the extension region. (*B*) Interaction of NY18 HA with the long α2-6 shows the loss of the critical contact of Asp-225 with the base region (as observed in the case of SC18 HA in *A*). (*C*) Interaction of AV18 HA with α2-3 in cone-like topology shows that HA interactions with cone-like topology involves contacts only with the Neu5Ac and Gal sugars at the base in contrast to that of the umbrella-like topology of long α2-6. Glu-190 and Gln-226 in AV18 are positioned to provide optimal contacts with these sugars. The side-chain conformation of Glu-190 in AV18 was assigned based on that of Glu-190 in APR34 HA–α2-3 cocrystal structure. (*D*) The differences in the key amino acid positions between SC18, NY18, and AV18 HAs in comparison with the ASI30 and APR34 HAs. The differences in the amino acid contacts with α2-3 and α2-6 are quantified by using buried solvent-accessible area calculations [supporting information (SI) Fig. 6].

Results

Molecular Interactions of SC18, NY18, and AV18 HAs with α2-3 and α2-6. Based on analysis of HA–glycan cocrystal structures, the HA–glycan interactions are characterized by using a cone-like and an umbrella-like glycan topology (11). The x-ray crystal structure of SC18 HA has been solved (13, 14), but the cocrystal structure of this HA with sialylated glycans remains unsolved. The structures of NY18 and AV18 HA were obtained by making the single Asp-225–Gly (for NY18 HA) and the additional NY18 + Asp-190–Glu mutation for AV18 *in silico*. The cocrystal structures of the related A/Swine/Iowa/15/30 (ASI30) and A/Puerto Rico/8/34 (APR34) H1N1 HAs with α2-3 and α2-6 glycans (13) enabled the investigation of molecular interactions between SC18, NY18, and AV18 with α2-3 and α2-6 oligosaccharides.

The umbrella-like topology is preferred by longer α2-6 oligosaccharides (tetrasaccharide and higher). The LSTc pentasaccharide [*N*-acetylneuraminic acid (Neu5Ac) α2-6Galβ1–4 *N*-acetylglucosamine (GlcNAc) β1–3Galβ1–4Glc] used in the APR34 and ASI30 HA–α2-6 cocrystal structures represents this long α2-6. Superimposition of these cocrystal structures and SC18 HA demonstrated that the contacts with long α2-6 oligosaccharide are divided into two regions. The base region involves contacts with the Neu5Acα2-6Galβ1- motif, and the extension region involves contacts with the -GlcNAcβ1–3Galβ1–4Glcβ1- motif. A highly conserved set of amino acids (Tyr-95, Ser/Thr-136, Trp-153, Thr-155, His-183, Leu/Ile-194) are involved in anchoring the Neu5Ac (Fig. 1). In the case of APR34 and SC18 HAs, both the backbone carbonyl oxygen and side chain of Asp-225 are positioned to interact with the Gal sugar in the base region. On the other hand, only the carbonyl oxygen of Gly-225 in ASI30 HA is positioned to interact with this Gal (Fig. 1). Highly conserved Lys-222 and Gln-226 are also positioned to interact with the base region. The critical amino acids involved in contacts with the extension region are Asp-190 (in SC18 and ASI30 HA), Gln-192 and Ser-193 (Asn-193 in APR34 HA). NY18 HA, the Asp-225–Gly mutant of SC18, shares an almost identical glycan binding site with that of ASI30 HA and therefore lacks the extra contact provided by the side chain of Asp-225 with Gal in the base region. In contrast, AV18 (the Asp-190–Glu/Asp-225–Gly double mutant of SC18) lacks the critical contacts

BIOCHEMISTRY

provided by both Asp-225 and Asp-190 to the base and extension regions, respectively. Among SC18, NY18, and AV18 HAs, SC18 HA provides the best contacts with the long α2-6 in the umbrella-like topology followed by NY18 HA.

Distinct from the umbrella-like topology, the cone-like topology can be adopted by both α2-3 and α2-6 [preferentially by short trisaccharide units such as Neu5Acα2-6Galβ1–4Glc (or GlcNAc)]. Unlike the two distinct regions of HA contacts found with the umbrella-like topology, the contacts with the cone-like topology primarily involve substitutions that center around a trisaccharide Neu5Acα2-3/6Galβ1–3/4Glc (or GlcNAc) motif as observed in the HA–α2-3 cocrystal structures. Specifically, Glu-190 and Gln-226, which are highly conserved across various avian HAs, are critically involved in making optimal contacts with the cone-like topology (Fig. 1). This observation is corroborated further by the disordered sugars beyond Neu5Ac in the ASI30 HA–α2-3 cocrystal structure because Asp instead of Glu at 190 in this HA lacks the contact with the α2-3. Superimposition of AV18 and APR34 HA, which both contain these critical amino acids, shows that AV18 HA makes optimal contacts with the cone-like glycan topology. Both SC18 and NY18 HAs lack the critical Glu-190 residue, and therefore their contacts with the cone-like glycan topology are less optimal when compared with AV18 HA.

Dose-Dependent Direct HA Binding to Representative α2-3 and α2-6 Oligosaccharides. Novel glycan array platforms have been developed to investigate HA–glycan interactions (15, 16). These arrays have provided important insights into α2-3 versus α2-6 binding specificity of various WT and mutant HAs. In these glycan array studies, high and low binding signals to the glycans within a single assay using saturating HA concentrations determine the glycan binding preference for a given HA. It is generally accepted that the glycan binding affinity for a single binding site on any glycan binding protein (such as a lectin) is low (typically in the high micromolar to millimolar range). Because each HA unit is a trimeric protein, there are three glycan binding sites per unit (5). In addition, multiple HA units assemble on a virus surface. The glycan binding sites within a HA unit and the spatial arrangement of multiple HA units across a virus surface could play an important role in multivalent HA–glycan interactions. The concentration of the HA units relative to the glycans consequently will critically govern HA–glycan binding specificity.

To understand differences in the glycan binding specificity of SC18, NY18, and AV18 HAs for a specific spatial arrangement of the HA units and the glycans, systematic direct HA binding studies on a plate array were performed (see *Materials and Methods*). Minimal binding signals were observed for SC18 HA in the sequential ELISA-type binding assay (Fig. 2). Given that glycan spacing and HA unit size limits HA binding to only a single glycan in this assay, the binding signals are consistent with the anticipated weak affinity of the HA unit to a single glycan. The precomplexation assay with SC18 HA, where four HA units are locked spatially, instead resulted in at least an 8-fold increase in the binding to the long α2-6 glycan (Fig. 2). This dramatic increase in the binding signal underscores the role that the spatial arrangement of multiple HA units plays in enhancing glycan binding.

Dose-dependent direct binding assays by serial dilution of the precomplexed SC18, NY18, and AV18 HAs were performed to establish their relative glycan binding affinities (Fig. 3). The cooperativity factor n and the apparent binding constant K_d' were calculated based on the linearized Hill equation (see *Materials and Methods* and SI Fig. 7) used to model the binding data (Table 1). The R^2 value >0.95 for all of the glycan binding data indicates a good fit to the linearized Hill model. The value of $n \geq 1$ reflects the positive cooperativity in the HA–glycan interactions as a result of the spatial

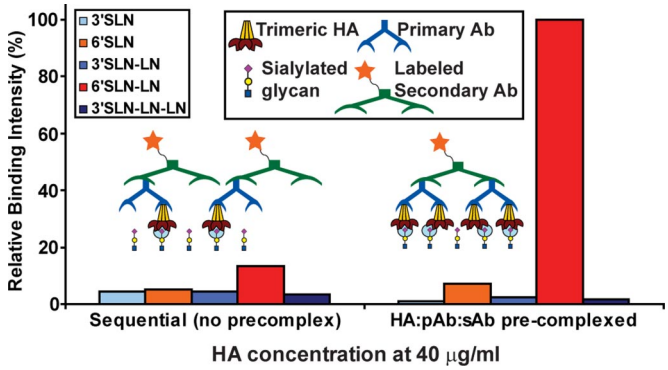

Fig. 2. Binding assay to capture multivalent HA–glycan interactions. Shown is a comparison of binding signals between sequential binding assay and precomplexation of HA units with primary (pAb) and labeled secondary (sAb) antibodies. The conditions of the sequential assay (see *Materials and Methods*) favor the formation of HA/pAb/sAb in a 1:1:1 ratio. Despite the abundance of the labeled sAb (1 per HA unit) the minimal binding signals observed even at a high HA concentration of 40 μg/ml supports the low affinity binding of a single glycan to a HA unit (cyan circle). On the other hand, the conditions for precomplexation of HA/pAb/sAb in a ratio of 4:2:1 favor the spatial arrangement of four HA units per precomplex. This spatial arrangement enhances the glycan binding signals via multivalency as shown by at least an 8-fold increase in binding to 6′SLN-LN given that there are four binding events (each event shown by a cyan circle) per precomplexed HA unit.

arrangement of multiple HA units and the binding of a HA unit to a single glycan. Whereas SC18 HA showed high binding affinity to the single long α2-6 glycan (K_d' = 5.5 pM), AV18 HA showed the reverse trend with almost no α2-6 binding and high α2-3 binding affinity (K_d' = 5 pM). On the other hand, whereas the long α2-6 binding of NY18 HA was almost identical to that of SC18 HA at saturating HA concentrations (Fig. 3), the binding affinity to long α2-6 (K_d' = 6 nM) was significantly lower than that of SC18 HA. These observations correlate with the differences in molecular interactions of SC18, NY18, and AV18 with α2-3 and α2-6 oligosaccharides.

Binding of SC18 and NY18 to Human Upper Respiratory Tissues. The remarkable differences in the binding affinities of α2-6 and α2-3 (from above) of SC18 and NY18 HA render them ideal lectin-like probes for investigating HA binding to diverse physiological glycans present in human upper respiratory tissues. Human tracheal sections were used to explore the binding pattern of SC18 and NY18 HA to the physiological glycans. Although both SC18 and NY18 bind to the apical side of the trachea (Fig. 4), the pattern and distribution of the tissue binding of the two HAs differ significantly. Notably, SC18 binding to the apical side of the trachea appears more restricted when compared with the well distributed binding of NY18. NY18 HA also shows binding to the internal region of the trachea (that are known to express α2-3 glycans), consistent with its direct binding to α2-3 glycans (Fig. 3). To further investigate the differences in apical binding of SC18 and NY18 HAs, costaining of tracheal tissues were performed with these HAs and Jacalin (a marker for goblet cells). This costaining demonstrated that whereas SC18 HA predominantly binds to goblet cells (expressing α2-6), NY18 HA showed minimal binding to these cells (Fig. 5).

Discussion

Glycan arrays comprising many distinct oligosaccharide motifs have been used to investigate the glycan binding of WT and mutant H1, H3, and H5 HAs (15–17). Despite these advances, interpretation of glycan receptor specificity that leads to human adaptation and transmission has remained challenging. This is caused, in large part, by a general notion that glycan–protein

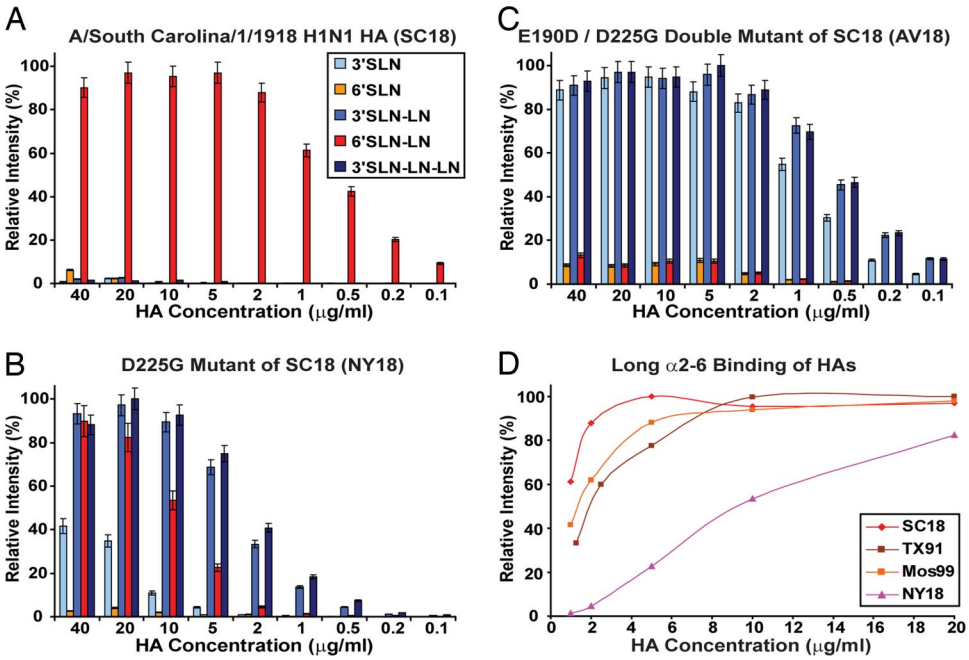

Fig. 3. Dose-dependent direct glycan binding of SC18, NY18, and AV18 HA. (*A–C*) The binding signals (expressed as percentage of maximum) of SC18, NY18, and AV18, respectively, in the dose-dependent direct binding assay. SC18 HA shows binding signals only to the long α2-6. At saturating HA concentrations (40 μg/ml), both SC18 and NY18 HA show identical binding to long α2-6, and NY18 HA also shows high binding signals to long α2-3. On the other hand, AV18 HA shows a reverse trend (in comparison with SC18 HA) of high-affinity α2-3 binding and minimal α2-6 binding. (*D*) Comparison of the long α2-6 (6′SLN-LN) binding of SC18, TX91, and Mos99 HAs with that of NY18 HA. Whereas the long α2-6 binding signal of NY18 HA approaches that of the other HAs at high concentrations, the binding curve of NY18 HA over the entire concentration range indicates that it has a dramatically lower long α2-6 binding affinity. Human-adapted SC18 and TX91 H1N1 viruses transmit efficiently in the ferret model (12). Human-adapted Mos99 H3N2 virus is a vaccine strain.

interactions are relatively weak and nonspecific. Consequently, the glycan binding specificity for HA has largely been established by using very high protein concentrations. High HA concentration may be useful to establish binders versus nonbinders but it imposes serious limitations on defining appropriate quantitative measurements to establish relative glycan binding affinities of HA. For example, at high concentrations, the typically used first-order binding kinetics assumptions (pertaining to HA/glycan ratio) would not be satisfied. To accurately quantify the relative glycan binding affinities between HAs, it is essential to be at the "appropriate" HA concentration range. Several key parameters, which include the spatial arrangement of multiple HA units, the surface glycan density (such as on a plate versus printed array), and the ratio of HA to glycan need to be taken into account when determining the appropriate HA concentration range for a given glycan array assay. Furthermore, comparing the glycan binding of different HAs at any single concentration point does not accurately capture the binding specificity that is established over a concentration range. In this study, the specific spatial arrangement of the glycans (spacing imposed by biotin-avidin system) and the HA (imposed by precomplexation of HA units) in tandem with the dose-dependent glycan binding assay was able to overcome these challenges. Most importantly, the concentration range used to determine the binding affinity parameters (n and K_d') is such that the glycan is in excess of the HA as would be expected in physiological conditions. This point is important for not only HA–glycan interactions, but also for glycan binding proteins in general. The observations presented in this study call for the reconsideration of the published results on glycan specificity based on high protein concentrations. The

Table 1. Quantifying the relative α2–3 and α2–6 binding affinities of SC18, NY18, and AV18 HAs

	6′SLN-LN		3′SLN-LN	
H1N1 HAs	n	$K_{d'}$	n	$K_{d'}$
SC18	1.3	5.5 pM	n.b.	n.b.
NY18	1.2	6.3 nM	1.3	50 pM
AV18	0.9	1 μM	1.3	5 pM

Relative binding affinities of SC18, NY18, and AV18 HAs to representative long α 2–3 and α 2–6 glycans. n.b. indicates no binding. The parameters n and $K_{d'}$ were determined as described in *Materials and Methods* and elaborated in SI Fig. 7. These parameters were obtained to purely quantify the relative binding affinities of the HAs, and hence their absolute values should be viewed only in this context.

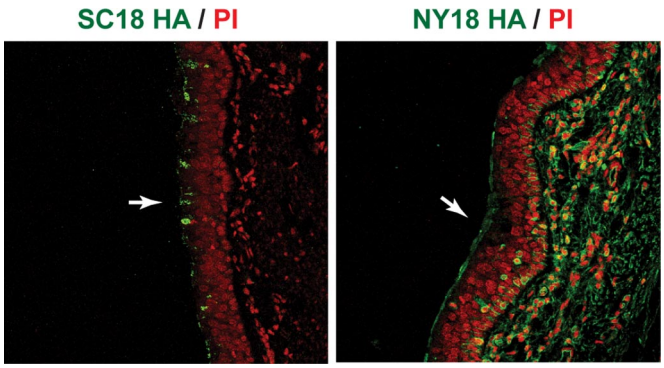

Fig. 4. Binding of SC18 and NY18 HA to human tracheal sections. The apical side of the tracheal epithelia is indicated by white arrows. The binding pattern of SC18 HA is localized around specific regions on the apical side; on the other hand, NY18 HA shows well distributed apical binding pattern (HA in green against PI in red). Furthermore, NY18 HA also shows significant staining on the inner regions of the epithelia that express α2-3 glycans (indicated by MAL-II-staining patterns) (data not shown). (Magnification: ×25.)

BIOCHEMISTRY

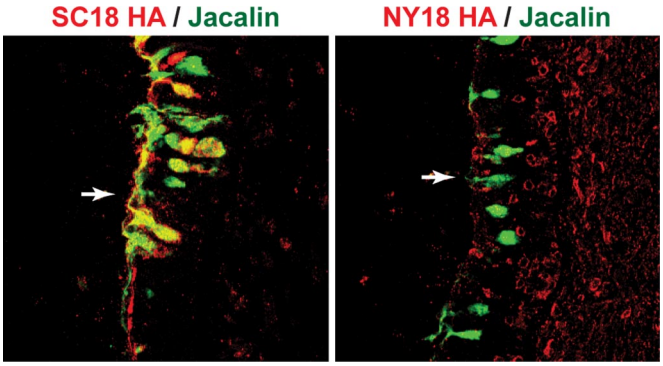

Fig. 5. Human tracheal costaining of SC18 and NY18 HA with Jacalin. The apical side of the tracheal epithelia is indicated by white arrows. The distinct apical binding patterns of SC18 and NY18 (in Fig. 4) are further elaborated by costaining the HAs (red) with Jacalin (green), a marker for goblet cells. The images were taken at ×25 magnification, and representative regions of the apical side are enlarged for clarity. The significant costain of SC18 HA with Jacalin (yellow) indicates that SC18 HA predominantly binds to goblet cells on the apical side of the epithelia. On the other hand, the binding pattern of NY18 HA has minimal overlap with that of Jacalin, indicating that it does not bind to goblet cells on the apical side of tracheal tissue.

approach described here can be readily extended to any glycan array platform to quantitatively investigate protein–glycan interactions.

At high HA concentrations, SC18 and NY18 HA display no differences in their binding to long α2-6 glycan. The only difference between SC18 and NY18 at saturating HA concentrations is the additional binding to α2-3 glycans for NY18 HA. As the α2-3 binding of SC18, NY18, and AV18 shows inverse correlation with the transmissibility, a probable conclusion from these data are that the loss of α2-3 binding specificity is a critical factor for transmission. However, A/Texas/36/91 (TX91), a mixed α2-6/α2-3 binding virus similar to NY18, transmitted efficiently in ferrets (12). The dose-dependent direct binding of TX91 and A/Moscow/10/99 H3N2 (Mos99; a mixed α2-6/α2-3 binding human-adapted H3 HA) compared with that of SC18 and NY18 clearly shows that the high affinity binding to long α2-6 glycan is a common feature for SC18, Tx91, and Mos99, but not for NY18 (Fig. 3). This common feature of specificity to long α2-6 glycan is independent of specificity to α2-3 glycans. Thus, this study corroborates the observation that the high-affinity binding to long α2-6 glycans, which are extensively expressed in the upper respiratory tissues, is a critical determinant not only for HA human adaptation, but also for influenza virus transmission.

The critical role of the long α2-6 glycans as physiological targets for influenza A virus infection and transmission also highlights the role of biosynthetic enzymes involved in synthesizing these glycans in addition to the α2-6 sialyltransferases. Specifically, the β4GalTs (β1–4 galactosyltransferases) and β3GlcNAcTs (β1–3 *N*-acetylglucosaminyl transferases) are involved in synthesizing multiple lactosamine repeats characteristic of long α2-6 glycans. The regulation of the expression of these glycosyltransferases would not only play a critical role in the viral tropism but it would also enable better selection pressure strategies to understand the evolution of mutations in HA that would lead to efficient human adaptation and human-to-human transmission.

Differential binding of SC18 and NY18 to the diverse physiological glycans present in the human upper respiratory tissues further substantiates the direct binding studies. The narrow binding of SC18 to goblet cells motivates future investigations into the cellular tropism of human-adapted viruses. This observation is consistent with a report by Matrosovich *et al.* (18), who demonstrated that human-adapted H1 and H3 virus strains preferentially infect nonciliated cells and avian viruses preferentially infect ciliated cells. They also suggested that such differences in the cellular tropism of the viruses could explain the differences in their efficiency of human–human transmission. Furthermore, the binding of SC18 HA to goblet cells taken together with its long α2-6 binding specificity correlates with its localized binding to the apical side of the tracheal tissue and also suggests the expression of long α2-6 glycans in the goblet cells. On the other hand, SNA-I that binds to both short and long α2-6 glycans shows more extensive apical side tracheal binding (11). Therefore, SC18 HA could potentially be a more effective lectin-like probe for investigating the distribution of long α2-6 as compared with SNA-I.

In conclusion, we have shown how quantitative differences in the HAs binding to long α2-6 glycans correlate with the observed differences in viral transmission. The study of the 1918 viruses varying only in their HA genes and having different transmission efficiencies served as a good model system for establishing this correlate. Given the potential threat of a pandemic from currently circulating avian H5N1 viruses, the approach presented here can aid in the screening of H5N1 HA mutants that could lead to human adaptation and transmission of these deadly viruses.

Materials and Methods

Cloning, Baculovirus Synthesis, Expression, and Purification of HA. The soluble form of HA was expressed by using the baculovirus expression vector system (BEVS). SC18 baculovirus [generated from pAcGP67-SC18-HA plasmid (14, 15)] was a gift from James Stevens (Centers for Disease Control). pAcGp67-NY18-HA and pAcGp67-AV18-HA plasmids were generated from pAcGP67-SC18-HA by [Asp-225–Gly] and [Asp-190–Glu, Asp-225–Gly] mutations respectively. Mutagenesis was carried out with the QuikChange multi site-directed mutagenesis kit (Stratagene). The primers used for mutagenesis were designed by using the web-based program, PrimerX (http://bioinformatics.org/primerx) and synthesized by IDT DNA Technologies. NY18 and AV18 baculoviruses were created from pAcGP67-NY18-HA and pAcGP67-AV18-HA constructs by using the Baculogold system (BD Biosciences) according to the manufacturer's instructions. The baculoviruses were used to infect 300-ml suspension cultures of Sf9 cells (BD Biosciences) cultured in BD BaculoGold Max-XP Insect Cell medium (BD Biosciences). These cultures were monitored for signs of infection and harvested 4–5 days postinfection. BEVS produces trimeric HA, which provides multivalent binding to glycans. The soluble form of HA was purified from the supernatant of infected cells as described (14). Briefly, the supernatant was concentrated by using Centricon Plus-70 centrifugal filters (Millipore), and the trimeric HA was recovered from the concentrated cell supernatant by using affinity chromatography with columns packed with Ni-NTA beads (Qiagen). Eluting fractions that contained HA were pooled and dialyzed overnight with a 10 mM Tris·HCl, 50 mM NaCl buffer (pH 8.0). Ion exchange chromatography was then performed on the dialyzed samples by using a Mono-Q HR10/10 column (GE Healthcare). The fractions containing HA were pooled together and subjected to ultrafiltration by using Amicon Ultra 100 K NMWL membrane filters (Millipore). The protein was then concentrated and reconstituted in PBS. The purified protein was quantified by using Bio-Rad's protein assay.

Dose-Dependent Direct Glycan Binding of HA. To investigate the multivalent HA–glycan interactions a streptavidin plate array comprising representative biotinylated α2-3 and α2-6 (short and long) was used. The spatial arrangement of the glycans in the wells of this plate array favors binding to only one of the three HA monomers in the HA unit. The glycan spacing and the HA unit size limit binding of the HA unit to a single glycan in the ELISA-type binding assay, which involves the sequential application of HA unit, primary and secondary antibodies (see below). Conversely, the precomplexation of HA units (see below) with primary and secondary antibodies (HA/primary/secondary = 4:2:1 ratio) facilitates a specific spatial arrangement of four HA units. This precomplexed unit therefore enabled the investigation of the effects of the relative spatial positioning of multiple HA units on the glycan binding affinity via multivalency.

Streptavidin-coated high binding capacity 384-well plates (Pierce) were loaded to the full capacity of each well by incubating the well with 50 μl of 2.4 μM biotinylated glycans overnight at 4°C. The biotinylated glycans [α2-3 sialylated lactosamine (3′SLN), α2-6 sialylated lactosamine (6′SLN), 3′SLN-LN,

6′SLN-LN and 3′SLN-LN-LN] were obtained from the Consortium of Functional Glycomics (www.functionalglycomics.org) through their resource request program. LN corresponds to lactosamine (Galβ1–4GlcNAc) and 3′SLN and 6′SLN correspond to Neu5Acα2-3 and Neu5Acα2-6 linked to LN, respectively. Excess glycans were removed through extensive washing with PBS. For the ELISA-type sequential binding, the glycan-coated wells were incubated for 2 h with HA at a concentration of 40 μg/ml (typical high concentrations used in glycan array experiments) in PBS containing 1% BSA and subsequently washed extensively with PBS-Tween followed by PBS. This process was followed by incubation with the primary antibody (mouse anti 6× His tag IgG) at a concentration of 5 μg/ml in PBS containing 1% BSA for 3 h at room temperature and repeating the above wash steps. The wells were finally incubated with a 2 μg/ml solution of the secondary antibody (HRP-conjugated goat anti mouse IgG) for 1 h at room temperature. In the case of dose-dependent precomplexed HA experiments, a stock solution containing appropriate amounts of His-tagged HA protein, primary antibody (mouse anti 6× His tag IgG) and secondary antibody (HRP-conjugated goat anti mouse IgG (Santa Cruz Biotechnology) in the ratio 4:2:1 and incubated on ice for 20 min. Appropriate amounts of precomplexed stock HA were diluted to 250 μl with 1% BSA in PBS. Fifty microliters of this precomplexed HA was added to each of the glycan-coated wells and incubated at room temperature for 2 h followed by the above wash steps. The binding signal was determined based on HRP activity by using Amplex Red Peroxidase Assay (Invitrogen) according to the manufacturer's instructions. Appropriate negative controls were included, and all assays were performed in triplicate.

Previously, dose-dependent direct binding assays using the above precomplexation were performed to establish binding specificity of human-adapted HAs to long α2-6 (11). These assays were performed by incubating different concentrations of HA with appropriate concentrations of primary and secondary antibodies (to achieve the 4:2:1 ratio stated above). However, in this method of precomplexation, the binding kinetics potentially limit the formation of HA precomplex at low HA concentrations (<5 μg/ml). To accurately quantify the relative binding affinities, it is important to be able to measure binding of the precomplex at a lower concentration range (0.05 to 5 μg/ml) (SI Fig. 8). Toward addressing this issue, the binding assay was modified by preparation of the precomplex at high HA concentration followed by serial dilution of the stock (as described above).

To quantify the binding affinity (for the above precomplexation assay), binding parameter K_d' is defined and calculated based on the following model. The typical form of the Hill equation is used to represent the multivalent binding

$$y = \frac{[\mathrm{HA}]^n}{[\mathrm{HA}]^n + K_d'}. \qquad [1]$$

Linearizing Eq. **1** gives

$$\log\left(\frac{y}{1-y}\right) = n^*\log([\mathrm{HA}]) - \log(K_d'), \qquad [2]$$

where y is the fractional saturation of the glycan binding sites in the HA units; [HA] is the concentration of HA (in M); n is the cooperativity factor; and K_d' is the apparent binding constant for the multivalent HA–glycan interactions. The value of y is calculated by normalizing the binding signals to the saturating binding signal, which represents 100% occupancy on all HA units. n and K_d' were calculated based on the linearized Hill model (SI Fig. 7). An important assumption in the above model is that the glycans in each well of the plate are in excess of HA. To satisfy this assumption, the binding signals for HA concentration range from 0.05 to 5 μg/ml was used to calculate n and K_d'.

Binding of H1 HA to Human Upper Respiratory Tissues. Formalin-fixed and paraffin-embedded normal human tracheal tissue sections were purchased from US Biological. Tissue sections were deparaffinized, rehydrated, and preblocked with 1% BSA in PBS for 30 min at room temperature. HA–antibody precomplexes were generated by incubating recombinant SC18 and NY18 proteins with primary (mouse anti 6× His tag; Abcam) and secondary (Alexa Fluor-488 goat anti-mouse IgG; Invitrogen) antibodies in a ratio of 4:2:1, respectively, for 20 min on ice. The complexes formed were then diluted in 1% BSA-PBS to different final HA concentrations. Tissue binding studies were performed by incubating tissue sections with the diluted HA–antibody complexes for 3 h at room temperature. To visualize the cell nuclei, sections were counterstained with propidium iodide (PI) (Invitrogen; 1:100 in TBST) for 20 min at room temperature. For costaining assays, tissues were deparaffinized, rehydrated, and coincubated with FITC-labeled Jacalin [Vector Labs; 10 μg/ml in PBS with 0.05% Tween 20 (PBST)] and HA–antibody precomplexes (generated as described above with Alexa Fluor-546 goat anti-mouse IgG as secondary antibody and diluted in PBST) for 3 h at room temperature. Sections were then washed and viewed under a Zeiss LSM510 laser scanning confocal microscope.

ACKNOWLEDGMENTS. We thank Dr. James Stevens for providing the SC18 and Mos99 baculoviruses and pAcGP67-SC18-HA clone, the Consortium for Functional Glycomics for the supply of glycans for direct binding experiments, Dr. Shu-hua Nong for help with purification of the HA proteins, and Ms. Ada Ziolkowski for help with the preparation of the manuscript. Confocal microscopy was performed at the W. M. Keck Foundation Biological Imaging Facility at the Whitehead Institute (Cambridge, MA). This work was supported by the National Institute of General Medical Sciences Grant U54 GM62116, National Institutes of Health Grant GM57073, and the Singapore–Massachusetts Institute of Technology Alliance for Research and Technology, Singapore.

1. Tumpey TM, *et al.* (2005) Characterization of the reconstructed 1918 Spanish influenza pandemic virus. *Science* 310:77–80.
2. Kuiken T, *et al.* (2006) Host species barriers to influenza virus infections. *Science* 312:394–397.
3. Russell RJ, *et al.* (2006) Avian and human receptor binding by hemagglutinins of influenza A viruses. *Glycoconj J* 23:85–92.
4. Shinya K, *et al.* (2006) Avian flu: Influenza virus receptors in the human airway. *Nature* 440:435–436.
5. Skehel JJ, Wiley DC (2000) Receptor binding and membrane fusion in virus entry: The influenza hemagglutinin. *Annu Rev Biochem* 69:531–569.
6. van Riel D, *et al.* (2006) H5N1 virus attachment to lower respiratory tract. *Science* 312:399.
7. Neumann G, Kawaoka Y (2006) Host range restriction and pathogenicity in the context of influenza pandemic. *Emerg Infect Dis* 12:881–886.
8. van Riel D, *et al.* (2007) Human and avian influenza viruses target different cells in the lower respiratory tract of humans and other mammals. *Am J Pathol* 171:1215–1223.
9. Nicholls JM, *et al.* (2007) Sialic acid receptor detection in the human respiratory tract: Evidence for widespread distribution of potential binding sites for human and avian influenza viruses. *Respir Res* 8:73.
10. Nicholls JM, *et al.* (2007) Tropism of avian influenza A (H5N1) in the upper and lower respiratory tract. *Nat Med* 13:147–149.
11. Chandrasekharan A, *et al.* (2008) Glycan topology determines human adaptation of avian H5N1 virus hemagglutinin. *Nat Biotechnol* 26:45–51.
12. Tumpey TM, *et al.* (2007) A two-amino acid change in the hemagglutinin of the 1918 influenza virus abolishes transmission. *Science* 315:655–659.
13. Gamblin SJ, *et al.* (2004) The structure and receptor binding properties of the 1918 influenza hemagglutinin. *Science* 303:1838–1842.
14. Stevens J, *et al.* (2004) Structure of the uncleaved human H1 hemagglutinin from the extinct 1918 influenza virus. *Science* 303:1866–1870.
15. Stevens J, Blixt O, Paulson JC, Wilson IA (2006) Glycan microarray technologies: Tools to survey host specificity of influenza viruses. *Nat Rev Microbiol* 4:857–864.
16. Kumari K, *et al.* (2007) Receptor binding specificity of recent human H3N2 influenza viruses. *Virol J* 4:42–53.
17. Stevens J, *et al.* (2006) Structure and receptor specificity of the hemagglutinin from an H5N1 influenza virus. *Science* 312:404–410.
18. Matrosovich MN, *et al.* (2004) Human and avian influenza viruses target different cell types in cultures of human airway epithelium. *Proc Natl Acad Sci USA* 101:4620–4624.